# A SIMPL Model of Phage-Bacteria Interactions Accounting for Mutation and Competition

Carli Peterson[1], Darsh Gandhi[1], Austin Carlson[1], Aaron Lubkemann[1], Emma Richardson[1], John Serralta[3], Michael S. Allen[3], Souvik Roy[1], Christopher M. Kribs[1,2], Hristo V. Kojouharov[1*]

[1]Department of Mathematics, The University of Texas at Arlington, 411 S Nedderman Dr, Arlington, 76019, TX, USA.
[2]Department of Teacher and Administrator Preparation, The University of Texas at Arlington, 701 Planetarium Pl, Arlington, 76019, TX, USA.
[3]Department of Microbiology, Immunology, and Genetics, The University of North Texas Health Science Center, 3500 Camp Bowie Blvd, Fort Worth, 76107, TX, USA.

*Corresponding author(s). E-mail(s): hristo@uta.edu;
Contributing authors: cxp4986@mavs.uta.edu; dxg5343@mavs.uta.edu; ajc4834@mavs.uta.edu; asl1499@mavs.uta.edu; ecr9244@mavs.uta.edu; johnserralta@gmail.com; Michael.Allen@unthsc.edu; souvik.roy@uta.edu; kribs@uta.edu;

**Abstract**

*Pseudomonas aeruginosa* is an opportunistically pathogenic bacteria that causes fatal infections and epidemics in hospital environments. Due to the growing prevalence of antibiotic-resistant strains of *P. aeruginosa*, looking for alternative therapies is crucial. Bacteriophage therapy is emerging as a promising solution; however, it has not been approved for human clinical use and suffers from a lack of understanding of the complex dynamics between bacterial cells and phage virions. Mathematical models provide insight into these dynamics. Through a system of ordinary differential equations, we determined appropriate biological assumptions to effectively capture the complex dynamics observed between susceptible, infected, and mutated bacterial cells with bacteriophage virions in a microwell setting. Data fitting based on this model produced a set of parameter estimates unique to our experimental observations of a specific phage and *P. aeruginosa* strain. In translating observed optical density readings into bacterial

concentrations, we also found that bacterial debris has a significant impact on optical density, with a lysed bacterium contributing roughly **40%** as much to optical density readings as a living cell.

**Keywords:** Pseudomonas aeruginosa, optical density, bacterial dynamics, ranked competition, bacterial debris

# 1 Introduction

In the United States alone, more than 51,000 healthcare-associated *Pseudomonas aeruginosa* infections occur each year (Solomon and Oliver, 2014). Of these, roughly 13% are multidrug-resistant and are the primary cause of death for around 400 people annually (Solomon and Oliver, 2014). With the growing prevalence of resistant bacteria, the medical community is quickly entering a "post-antibiotic era"; hence, the necessity to overcome drug resistance is becoming increasingly urgent.

*Pseudomonas aeruginosa* is a common nosocomial pathogen that abides in sewage-contaminated areas, hospitals, and other locations frequented by humans (Bédard et al., 2016; Crone et al., 2019; Schroth et al., 2018). Infection from this pathogen can result in many different fatal diseases and is the lead cause of mortality in patients with cystic fibrosis (Blanchard and Waters, 2019; LiPuma, 2010; Malhotra et al., 2019; Serralta, 2023). Additionally, 10% of all hospital-acquired infections are *P. aeruginosa* affiliated, which doubles a patients' mortality rate (Pachori et al., 2019; Vincent et al., 2009). Due to the increasing antibiotic resistance and the severity of infections caused by *P. aeruginosa*, the World Health Organization has designated the development of an alternative treatment method a critical target (Tacconelli et al., 2018). Though bacteriophages were first introduced as a treatment for infections in the United States during the 1920s, antibiotic production surged in the 1940s. As a result, antibiotics dominated as the primary method for treating infection, leaving bacteriophage therapeutics widely unused for decades. With *P. aeruginosa* showing strong resistance to common antibiotics such as beta-lactams, fluoroquinolones, and aminoglycosides in recent years, remedies involving bacteriophages have re-emerged as promising alternatives to these traditional treatments (Chegini et al., 2020).

Bacteriophages, also known as phages, are viruses consisting of a DNA or RNA genome enclosed in a protein capsid that infect and replicate in bacterial cells (Serralta, 2023). Found in soil, marine ecosystems, and the human body, these virions are the most plentiful, diversified predators on the planet (Łusiak-Szelachowska et al., 2020). For every one bacterium, there are an estimated ten phage virions in the world (Clokie et al., 2011). The sheer abundance of bacteriophages makes phage therapy incredibly promising.

Bacteriophages can be grouped according to two distinct lifestyles. Virulent phages that exclusively utilize the lytic cycle and temperate phages that can utilize both the lytic and lysogenic cycles. Lytic phages attach to the surface of a host cell through surface receptors and inject their prophage (genetic material) into the cytoplasm of the bacterial cell. This allows the phage to hijack the machinery of the cell to create

new phage components. They then lyse the cell, expelling new phage particles into the environment (much like bursting a piñata at a birthday party). On the other hand, in addition to a lytic lifecycle, lysogenic phages can alternatively attach to a host cell and incorporate their nucleic acid into the chromosome of the cell. By doing so, these so called prophages lay dormant and replicate with the cell DNA to be passed on to subsequent bacterial generations. After a delay known as the latent period, external stimuli trigger excision of the prophage from the host genome and commencement of the lytic cycle. Unlike chemotherapy or antibiotics which simply aim to kill bacterial cells, both lytic and lysogenic phages not only destroy bacterial cells, but release a new generation of phage, expediting the healing process.

The current (lack of) understanding of bacteriophages leaves much to be desired before bacteriophage therapy can be ethically and practically prescribed outside of emergency authorizations. For example, bacteriophage are highly selective between host organisms, even between mutliple strains of the same species of bacteria. In a recent study, Kauppinen *et al.* (2021) tested a variety of bacteriophages against a commercial and an environmental *P. aeruginosa* strain and found no phage were lytic against both bacterial strains. Further, during the study, the PA01 *P. aeruginosa* strain developed resistance to a phage strain. Similarly, Kwiatek *et al.* (2017) found only 50% of the obligatory lytic bacteriophage they tested propagated despite their quick adsorption time and short latent period. Webb *et al.* (2003) found that a Pf1-like phage is involved in lysing *P. aeruginosa*. Wright *et al.* (2018) found a *P. aeruginosa* strain developed resistance to many bacteriophages in a short experiment. Furthermore, many quantifiable aspects of bacteriophage-bacteria interaction remain unknown. Although previous studies have tried to estimate them, we do not have a concrete understanding on phage adsorption rate, bacterial reproduction and mutation rates, or even burst size of second-generation bacteriophage after lysis, especially for *Pseudomonas aeruginosa* and its many associated antagonistic bacteriophages.

Previous mathematical models have explored the dynamics between bacterial cells and bacteriophages (Abedon, 2008; Cairns et al., 2009; Han and Smith, 2012; Simmons et al., 2018; Smith, 2008; Vidurupola, 2018). For example, Abedon (2008) explained how one can model phage-bacteria interaction using continuous models and incorporating factors such as the latent period, partial bacterial resistance, and vertical transmission of lysogenic phages. Han and Smith (2012) introduced time delay and found conditions for the persistence of phage-resistant bacteria. Simmons *et al.* (2018) found phage mobility in environments with bacterial biofilm is crucial for their survival using an agent based model. While these modeling decisions may capture the nature of phage-bacteria interaction realistically, they significantly complicate the mathematical modeling, making producing meaningful results more challenging.

Smith (2008) modified existing models of phage-bacteria interaction by incorporating a density-dependent phage attack rate, as well as the loss of phages due to adsorption in both infected and uninfected bacteria. From this modification, he was able to conclude that, given any initial bacterial population, there exists a phage dose capable of reducing the host population to an insignificant fraction of its initial level within the first latent period (although this dose may be impractical in therapeutic settings). Similarly, Vidurupola (2018) incorporated multiple phage attachment and

phage loss due to attachment to actively infected bacteria in extending a previously developed deterministic phage-bacteria model. However, Vidurupola's deterministic and stochastic models assume there is lysogenic infection due to bacteriophage, which is uncommon in certain *Pseudomonas aeruginosa* bacteriophage strains, such as the one (JS-1) used in this study. Cairns *et al.* (2009) also incorporated bacteria acquiring phage-resistance, but they failed to account for competition for resources between susceptible and mutated bacteria. Further, Abedon, Han, Simmons, Cairns, and Smith do not quantify bacterial debris, and while Vidurupola does, no previous study (to our knowledge) investigates its effect on optical density measurements.

Optical density is a quantitative, unitless measure that indicates the degree of light scattering through a sample, and is one of the easiest and most common methods of determining cell density in liquid cultures. However, because this method purely measures light, there is no differentiation between bacterial components, whether living cells or debris from lysis, causing the observed scattering. Previously, bacterial debris was not a point of focus in determining conversions from optical density, as studies did not incorporate phages, and had no debris to account for. This led to linear functions becoming widespread for optical density to bacterial calculations, as they are quick to compute and are generally accurate (Zhang et al., 2015). Further, functions converting optical density to bacterial count are confounded by variability between spectrophotometers. This is caused by different optical systems, optical configurations, or even temperature (Matlock, 2017; Zhang et al., 2015). As a result, laborious calibration of optical density to true cell counts has become widespread, with a study as recently as 2020 introducing new calibration protocols (Beal et al., 2020). However, these calibration protocols fail to capture the dynamics we wish to study, as if serial dilutions are made to count cells, phages may continue to attach, resulting in further cell lysis and unrepresentative data. This difficulty has led those investigating phage-bacteria dynamics to develop new methods for fear of the effect bacterial debris has on optical density (Egido et al., 2023). The phage-bacteria effect on optical density has been somewhat explored, albeit for the purpose of detecting phages, leading to a similar lack of accurate quantification of cell number over the course of the experiment. With the fast, simple, and automated nature of optical density measurements, modeling phage-bacteria dynamics accurately given optical density is imperative to generating the data needed to further explore the viability of phages as a therapeutic tool.

In this study, we aim to integrate the factors implemented by Smith (2008) and Vidurupola (2018) to develop a mathematical model that captures the complex interaction, as observed through optical density measurements, between a strain of *Pseudomonas aeruginosa* and a novel lytic bacteriophage, JS-1, isolated in wastewater. In this setting, one might ask: What assumptions are necessary to accurately capture the interaction between phages and bacterial cells in a controlled environment? In addition, how significantly does bacterial debris contribute to optical density readings? We address these questions through a mathematical model that accounts for the different characteristics of susceptible and mutated bacteria and the presence of bacterial debris in the environment. These inclusions yield a realistic representation of the interaction between the two species and provides insight into the effect of bacterial debris on optical density measurements, which very few studies have explored.

# 2 Methods

## 2.1 Data Acquisition and Processing

We consider optical density (OD) measurements (at 600nm) of samples of strain BAA-31 of *P. aeruginosa* and JS-1 phage in a 96-well plate with lid on a Bio-Tek Synergy 2 multimode plate reader over the span of 18 hours with medium shaking and incubation at 37°C. *P. aeruginosa* BAA-31 was purchased from ATCC. Phage JS-1 was isolated from a wastewater sample collected in Azle, Texas (Serralta, 2023). Six experiments were conducted, in each of which varying amounts of the JS-1 phages (from $10^2$ through $10^6$ plus a phage-free control) were added, while the initial concentration of bacterial cells (obtained by diluting an overnight culture to an OD of 0.02) remained constant between tests. Three trials were run for each experiment, and OD measurements were taken every thirty minutes, providing us a total of 37 time points for each trial in all six experiments. The mean OD across trials was used for each experiment.

In addition, a seventh experiment with neither bacteria nor phage was run to establish a baseline value for OD across all trials. This value, 0.09 OD, was then subtracted from the optical density values in all other experiments in order to obtain OD values induced by the bacteria. We further process the data by converting it to bacteria colony forming units (CFU $mL^{-1}$) using a conversion found by Kim (2012). Their conversion equates 1.0 OD to $2.04 \times 10^8$ CFU $mL^{-1}$.

After converting the averaged optical density data for each experiment to bacterial count (CFU $mL^{-1}$), we calculate the multiplicity of infection (MOI) for each experiment. MOI is the ratio of bacteriophage to susceptible bacterial cells, and is is found by dividing the initial number of phage by the initial number of susceptible bacteria times the volume of each microwell. The MOI values for each experiment are described in Table 1.

**Table 1** The multiplicity of infection (MOI) for each experiment.

| Experiment | Susceptible Bacteria ($\times 10^7$ CFU $mL^{-1}$) | Phage (PFU $mL^{-1}$) | MOI |
|---|---|---|---|
| Experiment 1 | 1.180 | 0 | 0 |
| Experiment 2 | 1.173 | $10^2$ | $8.528 \times 10^{-6}$ |
| Experiment 3 | 1.167 | $10^3$ | $8.576 \times 10^{-5}$ |
| Experiment 4 | 1.107 | $10^4$ | $9.041 \times 10^{-4}$ |
| Experiment 5 | 1.133 | $10^5$ | $8.829 \times 10^{-3}$ |
| Experiment 6 | 1.113 | $10^6$ | $8.987 \times 10^{-2}$ |

## 2.2 Modeling Assumptions

To model the dynamics of the interaction between *Pseudomonas aeruginosa* and the JS-1 bacteriophage populations, we use the following set of modeling assumptions:

- There is a homogeneous mixture of bacterial cells and bacteriophage (Serralta, 2023).

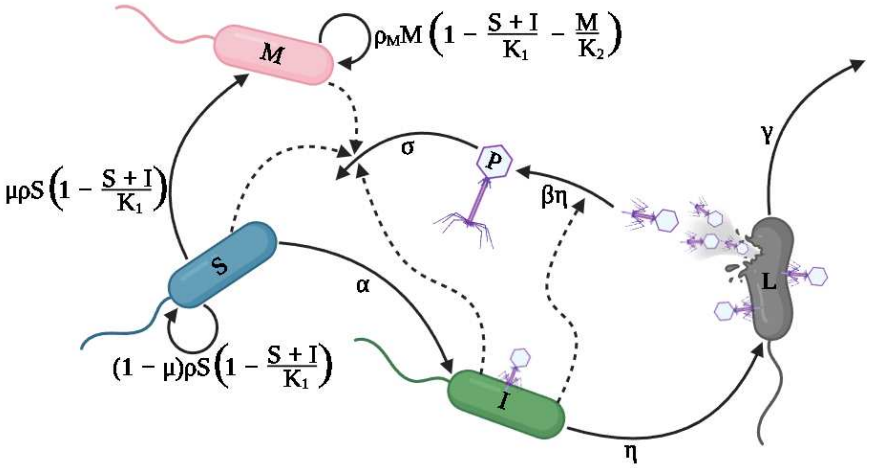



**Fig. 1** Visual representation of the dynamics between susceptible (S), infected (I), mutated (M), and lysed (L) bacteria and bacteriophages (P). Solid lines represent the transfer of an individual in or out of a population; dashed lines represent the influence of a population on a term. See Section 2.3 for a full explanation.

- Bacterial growth is limited by lack of nutrients and space (Kadurugamuwa and Beveridge, 1996; Ndongmo Teytsa et al., 2021).
- No natural death of the bacteria within the observed time frame (Emmanouilidou-Arseni and Koumentakou, 1964; Lewenza et al., 2018).
- Interactions between phage and bacteria are density-dependent (Han and Smith, 2012; Smith, 2008; Vidurupola, 2018).
- Multiple phage virions can attach to a single bacterial cell (Aksyuk et al., 2009; Bayer, 1968; Kokjohn and Sayler, 1991; Orlova, 2009).
- Bacterial cells can mutate to immunity from bacteriophage (nonpermissivity) (Barrangou et al., 2007; Booth et al., 1979; Burgener et al., 2019; Hynes et al., 2014), but trade-off survival factors such as motility and the composition of a bacterium's outer membrane (Mangalea and Duerkop, 2020; Serralta, 2023; Sinha et al., 2020).
- Both phage-susceptible and phage-resistant *Pseudomonas aeruginosa* cells can produce phage-resistant offspring (Barrangou et al., 2007; Booth et al., 1979; Burgener et al., 2019; Hynes et al., 2014).
- Phage-resistant bacteria cannot produce phage-susceptible offspring (Betts et al., 2014; Weitz et al., 2005).

## 2.3 The Mathematical Model

Incorporating the modeling assumptions, as discussed in Section 2.2, yields the following system of five ordinary differential equations:

$$
\begin{aligned}
\frac{\mathrm{d}S}{\mathrm{d}t} &= \underbrace{(1-\mu)\rho S\left(1-\frac{S+I}{K_1}\right)}_{\text{reproduction without mutation}} - \underbrace{\alpha S P}_{\text{infection}}, \quad S(0)=S_0,\\
\frac{\mathrm{d}I}{\mathrm{d}t} &= \underbrace{\alpha S P}_{\text{infection}} - \underbrace{\eta I}_{\text{burst}}, \quad I(0)=0,\\
\frac{\mathrm{d}M}{\mathrm{d}t} &= \underbrace{\rho_M M\left(1-\frac{S+I}{K_1}-\frac{M}{K_2}\right)}_{\text{reproduction}} + \underbrace{\mu\rho S\left(1-\frac{S+I}{K_1}\right)}_{\text{birth with mutation}}, \quad M(0)=M_0,\\
\frac{\mathrm{d}P}{\mathrm{d}t} &= \underbrace{\beta\eta I}_{\text{burst}} - \underbrace{\sigma(S+I)P}_{\text{infection}}, \quad P(0)=P_0,\\
\frac{\mathrm{d}L}{\mathrm{d}t} &= \underbrace{\eta I}_{\text{burst}} - \underbrace{\gamma L}_{\text{decay}}, \quad L(0)=0.
\end{aligned}
\tag{1}
$$

The state variables, *S, I, M, P, L*, represent susceptible (S), infected (I), and mutated (M) bacteria, free bacteriophage (P), and lysed (L) bacterial remains. In the experimental setup, all of the bacteria are *P. aeruginosa* and the bacteriophage are JS-1. Susceptible bacteria are those which have not interacted with any bacteriophage (Alharbi and Kribs, 2022; Ndongmo Teytsa et al., 2021), while each infected bacterium has at least one phage virion attached to its cell membrane. The mutated bacterial population represents *P. aeruginosa* cells which have gained immunity from the bacteriophage. The lysed population accounts for all dead bacterial cells. Recall that in our experimental setup, *P. aeruginosa* cells only die due to lysis from producing bacteriophage. This lysed cell equation is used primarily for data fitting since the rest of the system decouples from it, which helps us investigate how bacterial debris contributes to optical density measurements.

We model the growth of the susceptible population logistically, where $\rho$ ($\mathrm{hr}^{-1}$) is the reproductive rate and $K_1$ (CFU $\mathrm{mL}^{-1}$) is the carrying capacity of the susceptible and infected cells. In the absence of phage, the bacterial population grows exponentially until stabilizing at $K_1 > 0$ due to lack of nutrients (including oxygen) or space. The growth rate of the susceptible bacteria when growing to the carrying capacity is reduced by the existing bacterial populations (susceptible and infected), since those take up space and resources. However, note that infected bacteria do not reproduce before they lyse. A proportion, $\mu$ (dimensionless), of the new bacterial cells produced mutate to immunity from bacteriophage, meaning susceptible bacteria are produced at proportion $(1-\mu)$ of the logistic growth expression. Since phage-bacteria interaction is density-dependent, we use a mass action term to model this, where susceptible bacteria interact with phages at a rate $\alpha$ (mL $\mathrm{PFU}^{-1}$ $\mathrm{hr}^{-1}$).

Susceptible bacteria transfer to the infected compartment when a susceptible bacterium interacts with a bacteriophage. Infected bacteria then lyse at a rate $\eta$ ($\mathrm{hr}^{-1}$). As noted by Smith (2009), the lysis rate is the inverse of the latent period. The lysed

bacterial population increases at the same rate, $\eta$. This population decays at a rate $\gamma$ ($\text{hr}^{-1}$) as a lysed bacterial cell's membranes diffuse throughout the medium and are absorbed by other bacteria for nutrients. The mutated population grows when susceptible bacteria produce mutated offspring at a proportion $\mu$ of all susceptible bacterial offspring, and the mutated population reproduces logistically with reproduction rate $\rho_M$ ($\text{hr}^{-1}$). Since mutated bacteria compete for space and resources with wild-type bacteria, we incorporate ranked competition in our model, with mutated bacteria able to access only the space and resources not used by susceptible and infected bacteria, and a second, lower carrying capacity $K_2 < K_1$ (CFU $\text{mL}^{-1}$) for mutated bacteria (due to a hypothesized resistance/fitness tradeoff). The mutated bacterial population doesn't decrease since the experiment has a significantly shorter duration than the lifespan of *Pseudomonas aeruginosa* bacterium and since they are resistant to infection by free phage.

Since bacteriophage virions cannot reproduce by themselves, the phage population increases only as infected bacteria lyse. New phage are produced at a rate $\beta\eta$, where $\beta$ is the average burst size per lysed bacterium (PFU $\text{CFU}^{-1}$) and $\eta$ is the burst rate of the infected bacteria as before. Although bacteriophage do not die naturally, the phage population decreases at a rate $\sigma$ (mL $\text{CFU}^{-1}$ $\text{hr}^{-1}$), which represents phage virions interacting with and attaching to susceptible and infected bacteria. The interaction is modeled using a mass action term.

We also consider the total bacterial population, $B = S + I + M + \epsilon L$, which is the sum of the susceptible, infected, and mutated populations and the lysed population multiplied by a weight $\epsilon$ (dimensionless). The corresponding Equation (2):

$$\frac{dB}{dt} = (\rho S + \rho_M M)\left(1 - \frac{S+I}{K_1}\right) - \rho_M\left(\frac{M}{K_2}\right) - (1-\epsilon)\eta I - \epsilon\gamma L \tag{2}$$

is crucial for data-fitting. Once we convert the experimental optical density data to CFU $\text{mL}^{-1}$, we can compare the estimated experimental bacterial count to simulated bacterial count from Equation (2) for parameter estimation and data fitting. Further, we estimate $\epsilon$, which previous studies have not explored in the past.

Note that the susceptible, infected, and phage population equations in Model (1) do not depend on mutated or lysed bacterial cells. This results in Model (3), a subsystem $SIP$ of Model (1), which decouples from the $L$ and $M$ equations:

$$\begin{aligned}
\frac{\mathrm{d}S}{\mathrm{d}t} &= \underbrace{\rho S\left(1 - \frac{S+I}{K_1}\right)}_{\text{reproduction}} - \underbrace{\alpha S P}_{\text{infection}}, \\
\frac{\mathrm{d}I}{\mathrm{d}t} &= \underbrace{\alpha S P}_{\text{infection}} - \underbrace{\eta I}_{\text{burst}}, \\
\frac{\mathrm{d}P}{\mathrm{d}t} &= \underbrace{\beta\eta I}_{\text{burst}} - \underbrace{\sigma(S+I)P}_{\text{infection}}.
\end{aligned} \tag{3}$$

**Table 2** State variables and parameters for Model (1) with their descriptions and units.

| Parameters | Description | Units |
|---|---|---|
| $S$ | Susceptible Bacteria | CFU $mL^{-1}$ |
| $I$ | Infected Bacteria | CFU $mL^{-1}$ |
| $M$ | Mutated Bacteria | CFU $mL^{-1}$ |
| $P$ | Bacteriophage | PFU $mL^{-1}$ |
| $L$ | Lysed Bacteria | CFU $mL^{-1}$ |
| $B$ | Total Live and Lysed Bacteria | CFU $mL^{-1}$ |
| $\rho$ | Bacterial reproduction rate | $hr^{-1}$ |
| $\rho_M$ | Mutated bacterial reproduction rate | $hr^{-1}$ |
| $K_1$ | Carrying capacity of susceptible and infected bacteria | CFU $mL^{-1}$ |
| $K_2$ | Carrying capacity of mutated bacteria | CFU $mL^{-1}$ |
| $\alpha$ | Phage adsorption rate | mL $PFU^{-1}$ $hr^{-1}$ |
| $\eta$ | Lysis rate | $hr^{-1}$ |
| $\gamma$ | Lysed bacterial decay rate | $hr^{-1}$ |
| $\beta$ | Burst size | PFU $CFU^{-1}$ |
| $\sigma$ | Bacterial interaction rate | mL $CFU^{-1}$ $hr^{-1}$ |
| $\mu$ | Mutation rate | dimensionless |
| $\epsilon$ | Weight of contribution of bacterial debris to optical density | dimensionless |

All parameters for Model (1) are nonnegative and are listed in Table 2. To determine estimates for all parameters, we construct an optimization and data fitting problem as described in Section 2.4 and Section 4.1.

## 2.4 Optimization Model for Parameter Estimation and Model Evaluation

As discussed in Section 2.1, we consider six experiments mixing varying amounts of JS-1 bacteriophage with *Pseudomonas aeruginosa* BAA-31 in a microwell plate over 18 hours. Optical density (OD) of three microwells for each experiment was measured on-instrument every thirty minutes, and we average the OD values of the three trials of each experiment to obtain the OD for each experiment. One of the experiments featured bacteria in the microwell without any bacteriophage, while the rest included $10^2, 10^3, 10^4, 10^5$, and $10^6$ bacteriophage. We also acquired data from a seventh experiment with neither bacteria nor bacteriophage and subtracted the averaged OD value from that experiment from the rest of our OD data to account for the baseline OD measurement.

Model (1) incorporates lysed bacterial remains. We hypothesize that bacterial debris contributes to the optical density readings of each experiment at an unknown, smaller weight than live bacteria. Using the processed OD data for each trial, we set up a constrained optimization problem to estimate the parameters listed in Table 2, including $\epsilon$, the weight applied to the lysed bacterial population when considering its effect on optical density. Since a lysed bacterium has burst and is thus less dense, we know $0 \leq \epsilon < 1$.

To estimate our model parameters, we use a least-squares data fitting method detailed in Section 4.1. We minimized a functional $J(OD, \boldsymbol{\theta})$ (subject to Model (1)) while varying $\boldsymbol{\theta}$, the set of parameters. To solve this problem, we first numerically

solved Model (1) in MATLAB® using the `ode15s` solver and then used MATLAB's `MultiStart` algorithm to repeatedly run the `fmincon` optimization solver (MathWorks, 2024). We assessed the accuracy of our parameter estimates by calculating the relative $l^2$ error percentage as described in Section 4.2.

# 3 Qualitative Analysis

We begin our analysis of Model (1) by considering its possible end states, leaving an examination of the transient dynamics to numerical work in the following section. As noted in Section 2.3, Model (3) decouples from the $M$ and $L$ equations in System (1), and analyzing Model (3) provides insight into the dynamics of both the $SIP$ subsystem and the full $SIMPL$ system (1).

## 3.1 Analysis of Model (3)

We find the equilibria of Model (3) by setting the right-hand side of each equation equal to zero. The system then has the following equilibria:

1. the phage-free equilibrium (PFE): $S = K_1$, $I = 0$, $P = 0$;
2. a line of non-isolated bacteria-free equilibria (BFE): $S = 0$, $I = 0$, $P = x$, where $x \in \mathbb{R}^+$;
3. the coexistence equilibrium (COE):

$$S = K_1\left[\frac{ac-(ab-1)}{a^2bc}\right],\ I = K_1\left[\frac{(ac-(ab-1))(ab-1)}{a^2bc}\right],\ P = \frac{ab-1}{a},$$

where $a = \dfrac{\alpha}{\eta}$, $b = \dfrac{\beta\eta}{\sigma}$, and $c = \dfrac{\rho}{\alpha}$.

This last equilibrium exists (is nonnegative) if and only if $1 < ab < 1 + ac$. The lower inequality guarantees that phages propagate well, and the upper one that the bacteria survive.

Note that adjoining the BFE there is a trivial extinction equilibrium where susceptible and infected bacteria and free phage populations are at zero, but this only occurs when there are neither bacteria nor phage at the initial time.

Local stability can be studied via the Jacobian equilibrium. Detailed computations are shown in the Appendix. The following result identifies the stability condition $ab < 1$ for the PFE $(K_1, 0, 0)$.

**Theorem 1** *For Model (3), the phage-free equilibrium is locally asymptotically stable (LAS) if $\alpha\beta < \sigma$.*

Theorem 1 indicates that there is a bacterial "winning" scenario if the rate at which phage are produced ($\alpha\beta$) is less than the rate ($\sigma$) at which they attach to bacterial cells (thus being removed from circulation). In the long-term dynamics of this scenario, the susceptible bacterial population stabilizes at the carrying capacity $K_1$, while there are no phage or infected bacteria left.

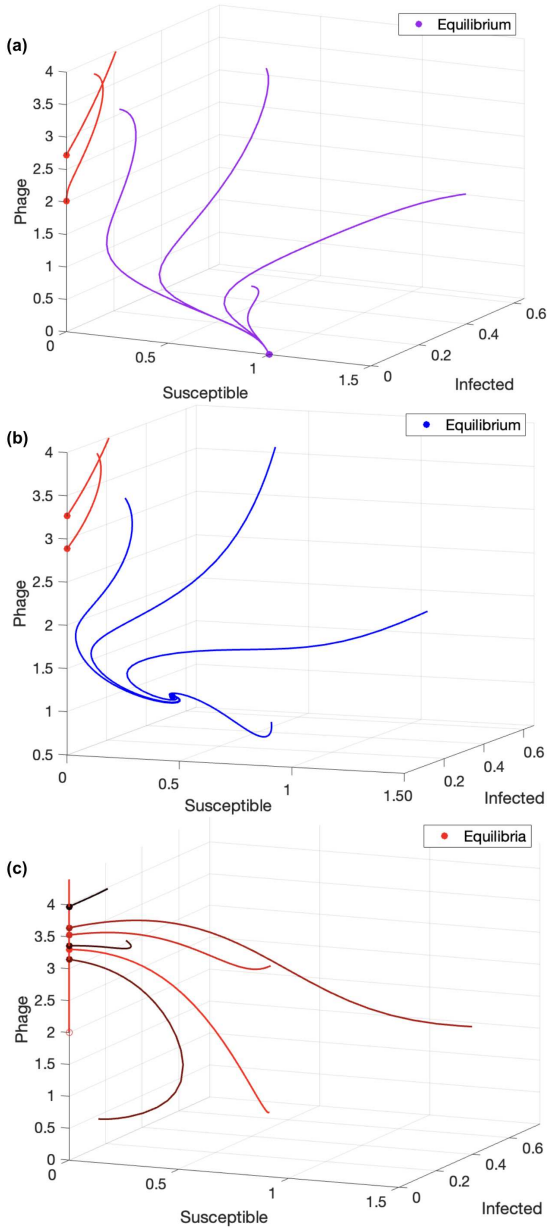



**Fig. 2** Long-term dynamics of susceptible, infected, and phage populations in Model (3), for the three cases $0 < ab < 1$, $1 < ab < 1 + ac$, and $1 + ac < ab$. For all three plots, a dot denotes a fixed point; shades of red represent "phage-win" scenarios, while purple a "bacterial-win" and blue coexistence. In (a), $\alpha\beta < \sigma$ so the phage-free equilibrium (PFE) is LAS. In (b), the coexistence equilibrium occurs and is LAS when $1 < \frac{\alpha\beta}{\sigma} < 1 + \frac{\rho}{\eta}$. In (c), there are no stable isolated equilibria, but in all three cases, the upper portion $P^* > c = \frac{\rho}{\alpha}$ of the line of bacteria-free equilibrium (BFE) is attracting, identified by an empty red circle along the phage axis at $\frac{\rho}{\alpha}$ and a red line extending upward from that point.

The non-isolated nature of the BFE $(0, 0, x)$ complicates their stability analysis, and prevents any of them from being LAS. However, it is seen that a secondary bifurcation occurs on the phage axis at the point where $x = \frac{\rho}{\alpha}$. The portion of the axis above this point, consisting of BFE with $x > \frac{\rho}{\alpha}$, is locally attracting, making those equilibria stable but not asymptotically stable, while the lower portion of BFE, with $0 \leq x < \frac{\rho}{\alpha}$, is repelling, making those fixed points unstable.

The more complicated analysis for the COE is summarized in the following result.

**Theorem 2** *For Model (3), the coexistence equilibrium exists and is locally stable if* $1 < \frac{\alpha\beta}{\sigma} < 1 + \frac{\rho}{\eta}$.

See Appendix A.4 for more details. Biologically, this compound inequality means that the phage reproduction number ($\frac{\alpha\beta}{\sigma}$, a measure of its ability to invade bacteria and replicate) must exceed 1 (so that the phage population persists), but not by more than the reproductive ratio of the permissible bacteria ($\frac{\rho}{\eta}$)—or else the phages will overcome the wild-type bacterial population. In the latter case, phage replication will also tail off as the susceptible bacterial population vanishes.

In shifting to consider the system's global behavior portrait, it is worth observing that solutions cannot grow unbounded. Note first that with $(S + I)' = \eta[acS(1 - \frac{S+I}{K_1}) - I]$, we have that $S + I > K_1 \Rightarrow (S + I)' < 0$, so any value above $K_1$ serves as an eventual upper bound for $S + I$. Then note that with $P' = \sigma[bI - (S + I)P]$, $P > b \Rightarrow P' \leq 0$—more specifically $P' < 0$ unless $S + I = 0$, in which case $P' = 0$ as we are at a BFE—we have that $\max(b, P(0))$ serves as an eventual upper bound for $P$.

Finally, we observe that the system's two bifurcations at $ab = 1$ and $ab = 1 + ac$ divide the parameter space into three regions: (1) $0 < ab < 1$, where the PFE is LAS and the upper portion of the BFE line is locally attracting; (2) $1 < ab < 1 + ac$, where the COE is LAS and the upper portion of the BFE line is attracting; and (3) $1 + ac < ab$, where there are no LAS equilibria but the upper portion of the BFE line is attracting. Numerical exploration turns up no more complicated behaviors, so in mode (1), $ab < 1$, the phages "die out" unless initially there are few bacteria and many phages, so that despite their relative inefficiency the phages wipe out the few bacteria and then "sit dormant." In mode (2), $1 < ab < 1 + ac$, the phages are efficient enough to persist while the bacteria are able to survive despite the phages' parasitism, unless (again) there are initially few bacteria and many phages, in which case the phages wipe out the bacteria. In mode (3), $ab > 1 + ac$, the bacteria cannot survive the phage parasitism/predation and are gradually eradicated no matter how many there are initially. Any therapeutic use of bacteriophages would clearly aim to operate in this last mode.

## 3.2 Analysis of Model (1)

The long term dynamics of Model (1) are similar to those of Model (3) discussed in Section 3.1. By a theorem of Thieme (1992), the behavior of Model (1) is asymptotic to that of the $SIP$ subsystem (Model (3)), with $S$, $I$, and $P$ replaced by their limiting values $S^*$, $I^*$, and $P^*$. Notice that when $S$ and $I$ are the constants $S^*$ and $I^*$, the

$M$ and $L$ equations become logistic and linear respectively, and each approaches a unique equilibrium asymptotically. This implies that whenever a solution of the $SIP$ subsystem approaches an equilibrium, the full system approaches a unique equilibrium. Thus, the possible end states are those identified in Section 3.1, supplemented with the values $L^* = \eta I^*/\gamma$ and

$$M^* = \frac{k}{2}\left(1 + \sqrt{1 + 4\frac{\mu\rho S^*}{k\rho_M K_2}}\right) K_2, \text{ where } k = 1 - \frac{S^* + I^*}{K_1}.$$

# 4 Quantitative Analysis

## 4.1 Parameter estimation

All parameters were estimated, as detailed in the next section, and are given in Table 3.

**Table 3** Estimated parameter values for bacteria and bacteriophage population dynamics

| Parameter | Description | Value | Units |
|---|---|---|---|
| $\rho$ | Susceptible bacteria reproduction rate | 0.5163 | $hr^{-1}$ |
| $\rho_M$ | Mutated bacterial reproduction rate | 0.7230 | $hr^{-1}$ |
| $K_1$ | Carrying capacity of susceptible and infected bacteria | $3.019 \times 10^8$ | CFU $mL^{-1}$ |
| $K_2$ | Carrying capacity of mutated bacteria | $1.328 \times 10^8$ | CFU $mL^{-1}$ |
| $\alpha$ | Phage interaction rate | $1.002 \times 10^{-2}$ | mL $PFU^{-1}$ $hr^{-1}$ |
| $\eta$ | Lysis rate | 0.6000 | $hr^{-1}$ |
| $\gamma$ | Lysed bacterial decay rate | $4.889 \times 10^{-3}$ | $hr^{-1}$ |
| $\beta$ | Burst size | $1.659 \times 10^2$ | PFU $CFU^{-1}$ |
| $\sigma$ | Bacterial interaction rate | $1.742 \times 10^{-2}$ | mL $CFU^{-1}$ $hr^{-1}$ |
| $\mu$ | Mutation rate | $4.886 \times 10^{-5}$ | dimensionless |
| $\epsilon$ | Weight of contribution of bacterial debris to optical density | 0.4312 | dimensionless |
| $\xi$ | Portion of initial bacteria with phage-resistance mutation | $5.665 \times 10^{-4}$ | dimensionless |

Using the optical density data acquired after pre-processing (as described in Section 2.1) and Model (1), we aimed to assess how heavily, if at all, lysed bacterial cells contribute to optical density readings. For the parameter estimation, we employed a least-squares data fitting method that is formulated as the following constrained optimization problem:

$$\min_{\boldsymbol{\theta} \in T_{ad}} J(OD, \boldsymbol{\theta}) := \frac{\omega}{2} \sum_{i=1}^{6} \sum_{j=1}^{N_t} (OD_i(t^j) - OD_i^j)^2 + \frac{\nu}{2}\|\boldsymbol{\theta}\|_2^2, \text{ subject to (1).} \quad (4)$$

Here, $\boldsymbol{\theta}$ represents the parameter vector that is estimated using the minimization problem (see Table 3), $OD_i^j$ is the measured optical density data at time point $t^j$,

$OD_i(t^j)$ is the estimated OD data using Model (1) with the initial conditions as

$$(S_i(0), I_i(0), M_i(0), P_i(0), L_i(0))$$

at the measured time point $t^j$, $N_t$ is the number of measurement times, and $T_{ad}$ is an admissible set of parameters defined as

$$T_{ad} = \{\boldsymbol{\theta} \in \mathbb{R}^n : \boldsymbol{\theta}_i^l \leq \boldsymbol{\theta}_i \leq \boldsymbol{\theta}_i^r\}$$

with $[\boldsymbol{\theta}_i^l, \boldsymbol{\theta}_i^r]$ representing the feasible range of the parameter $\boldsymbol{\theta}_i$. The initial condition $M_i(0)$ is estimated to be a small proportion, $\xi$ (dimensionless), of the starting number of bacterial cells. This amount is then subtracted from the original bacterial count to determine the initial number of susceptible bacteria, $S_i(0)$. The beginning number of infected and lysed bacteria are assumed to be zero across all experiments. The initial condition $P_i(0)$ corresponds to the starting number of phages added to the microwell plate in each experiment, as detailed in Sections 2.1 and 2.4. The functional $J$ consists of a data-fitting term with weight $\omega > 0$ and a regularization term with weight $\nu > 0$, where $\|\cdot\|_2$ represents the standard Euclidean norm of vectors in $\mathbb{R}^n$.

To solve Problem (4), we first use a forward Euler discretization to determine the numerical solution of the ODE (1). We then use the MATLAB® `fmincon` solver to perform the constrained minimization of $J$. The `fmincon` solver uses as default the interior-point optimization method (e.g, see Schmidt (2015)) to carry out the constrained optimization. This is an iterative method depending on an initial guess for $\boldsymbol{\theta}$ and yields a local minimum of $J$. We next employ the MATLAB® `MultiStart` solver to repeatedly run the `fmincon` solver with varying initial guesses of $\boldsymbol{\theta}$ and obtain the corresponding local minima parameter estimates. Amongst the different parameter estimates, we then choose the estimate that results in the least value of $J$.

## 4.2 Goodness of fit

We define the goodness of fit by the discrete relative $l^2$ error percentage (EP), as follows:

$$EP = \sqrt{\frac{\sum_{i=1}^{6}\sum_{j=1}^{N_t}(OD_i(t^j) - OD_i^j)^2}{\sum_{i=1}^{6}\sum_{j=1}^{N_t}(OD_i^j)^2}} \times 100.$$

The lower the value of EP, the better the model fits the data. In principle, we desire for a model fit with EP $< 10\%$.

Using the methods detailed in Section 4.1, we obtained an optimal set of parameter value estimates that fit our model to the given data with an EP of 8.5%. As seen in Fig. 3, our model fits the data well at the beginning of the experiments. However, for each experiment, the ending tends to lose the fit, which is where the resistant (mutated) bacterial population grows faster than predicted, by a factor dependent on the initial number of phages. This implies that our model lacks a mechanism to account for this relationship.

These results highlight the contribution of lysed bacteria to optical density measurements, indicated in Table 3 by the parameter $\epsilon$. Here we found $\epsilon$ to be 0.43, which

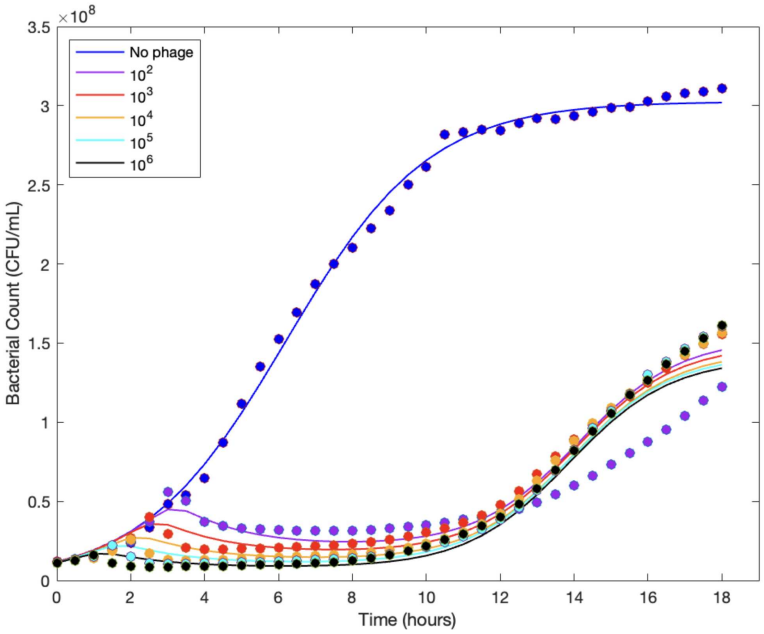



**Fig. 3** A calibration of Model (1) with parameter values detailed in Table 3, determined using the `MultiStart` algorithm. Solid lines represent simulated bacterial counts and dots represent estimated bacterial count from observed optical density data. Varying colors indicate experiments using different amounts of initial phage taken from the experimental data.

implies once a cell lyses, it loses roughly 60% of its contribution to optical density measurements. This contribution is significant and results in a much more accurate fit of our model to the data. Running our simulations disregarding the lysed bacterial contribution, we were only able to obtain an EP of 11%, compared to an EP of 8.5% with the debris included. With few previous studies considering the effect bacterial debris has on OD measurements, this finding will aid in future studies considering phage-bacteria dynamics observed through optical density measurements.

## 4.3 Numerical Results

In this section, we present numerical results, including details of our parameter estimates, and compare them to past studies and to our analysis of the dynamics of bacteria and phage populations. To obtain the parameter estimates listed in Table 3, we minimized functional $J$ from Problem (4). The cost functional $J$ consists of a tracking cost (multiplied by $\omega$) and a regularization cost (multiplied by $\nu$). For our parameter estimates, we used a tracking weight $\omega = 100$ and a regularization weight $\nu = 1$. We numerically solved Problem (4) using the methods described in Sections 2.4 and 4.1 to obtain our parameter estimates.

We found $\alpha$, the phage adsorption rate by susceptible bacteria, to be $1.002 \times 10^{-2}$ mL PFU$^{-1}$ hr$^{-1}$, and $\sigma$, the interaction rate with bacteria for bacteriophage, to be $1.742 \times 10^{-2}$ mL CFU$^{-1}$ hr$^{-1}$. Smith (2008) reported the value for phage adsorption to be about $0.9 \times 10^{-7}$ mL hr$^{-1}$. Smith also assumed bacteria grow exponentially and

unbounded, and determined the bacterial reproductive rate to be 0.3 $hr^{-1}$. We found our parameter values for $\rho$, the bacterial reproduction rate, to be 0.52 $hr^{-1}$ and $\rho_M$, the bacterial reproduction rate for mutated bacteria to be 0.72 $hr^{-1}$. Although one might expect a lower growth rate for mutated bacteria due to a fitness trade-off, Fink *et al.* (2023) noted in their study of the growth rates between wild-type and mutated bacteria that although mutant cells have a similar maximum growth rate, a lower carrying capacity value allows them to continue growing fast at lower concentrations of resources. We found the carrying capacity for permissive (nonmutant) bacteria, $K_1$, to be $3.019 \times 10^8$ CFU $mL^{-1}$, while the carrying capacity for nonpermissive (mutant) bacteria, $K_2$, to be much lower (around $1.328 \times 10^8$ CFU $mL^{-1}$). Cairns (2009) found bacterial growth rate to be about 0.3 $hr^{-1}$ and Yang *et al.* (2008) found *P. aeruginosa* doubling time to be between 100 and 200 minutes, corresponding to a reproductive rate between 0.3 and 0.6 cells per hour. The disparity between our parameter values and Smith's can be accounted for by differences in the media, temperature, aeration rate, and even the shape of the flask, all of which affect growth rates. In addition, his model incorporates a density dependent phage attack rate and investigates a relationship between *E. coli* and associated antagonistic bacteriophage strains.

In a different study of two *P. aeruginosa* bacteriophages of the *Pbunavirus* genus (vB_PaeM_V523 and vB_PaeM_V524), isolated from wastewater, Kauppinen *et al.* (2021) found a latent period of 50-55 minutes and a mean burst size of 124-134 PFU/infected cell. In our experimentation, the value $1/\eta$ represents the phage latent period, which we estimated to be 100 minutes, and the burst size, $\beta$, to be 166 phage per bacterium. This difference is likely due to the different genus of phage used, and the larger number of bacterial cells ($10^5$ CFU $mL^{-1}$ versus $10^8$ CFU $mL^{-1}$ used in our study). In previous studies, however, Smith (2008; 2009) estimated a burst size of 50–150 phage/bacterium and Simmons *et al.* (2018) estimated a burst size of 100, which are much closer to our results. Smith (2009) also found a higher lysis rate of 2.5 $hr^{-1}$ compared to our value of 0.6 $hr^{-1}$. Recall, however, he assumed unlimited exponential growth of bacteria, creating an artificial need for phages to "reproduce" quickly. We also determined $\alpha$, the rate at which bacteria adsorb phage virions, to be $1.002 \times 10^{-2}$ mL $PFU^{-1}$ $hr^{-1}$, while others such as Schrag and Mittler (1996) estimated it to be about $2 \times 10^{-8}$ mL $hr^{-1}$. This value, however, varies a lot between strains of the same bacteria, not to mention varying between different types of bacteria.

Our parameter estimates overall clearly mark the bacteriophage as successful in terms of the analysis in Section 3, as a quick computation shows $ab = 95.4 >> 1.86 = 1 + ac$, placing the model in the mode where all solutions approach equilibria free of permissive bacteria $(S, I)$. The details of the transient behavior are illustrated in the sample trajectory presented in Fig. 4. From its graphs, we gain insight into the behavior of each population (susceptible, infected, mutated, lysed, and bacteriophage) over the span of the trial. Clearly, for the bacterial populations, four key phases occur during our experiment when bacteriophage are present. First, the susceptible population increases. The duration of this phase depends on the number of initial phage; for $10^5$ phage at the beginning of the experiment, the susceptible population grows for about 1.5 hours. This period is shortened with more initial phage and lengthens when there are fewer initial phage. Second is the infection period. In this phase, the susceptible

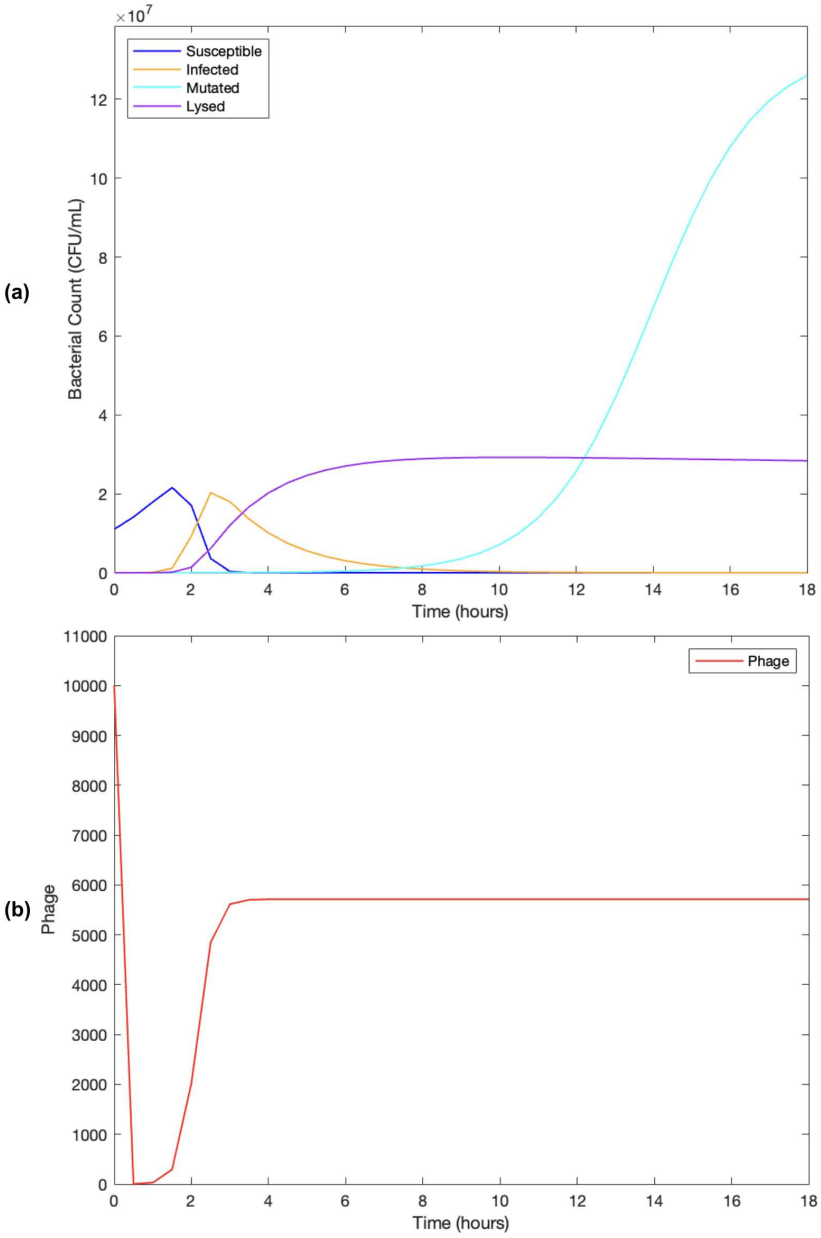



**Fig. 4** Numerical simulation of bacteriophage and susceptible, infected, mutated, and lysed bacterial populations over time using 10000 initial phage virions. In (a), the susceptible population is initially the biggest but dies off as they become infected by bacteriophage. Both the infected and susceptible eventually die off, leaving space for the mutated bacteria to compete for space and resources. In (b), the bacteriophage population quickly decreases as free phage attach to susceptible bacteria. The phage population then rebounds as infected bacteria lyse and then stabilizes after there are no more susceptible or infected bacteria to attach to.

population goes through a rapid decline due to phage adsorption, causing the infected population to increase. This period lasts 2-3 hours, depending on the size of the phage population. The third phase is the lysis period. During this phase, the infected cells lyse, producing free phage and bacterial debris. Subsequently, the phage and lysed populations boom before plateauing as the infected and susceptible populations completely die out. Finally, as the susceptible and infected bacteria die out, the mutant phase begins. Here, the mutant bacteria outcompete the dwindling susceptible and infected bacteria for resources and rapidly approach their carrying capacity. Outside of the 18-hour experiment timeframe, the mutated population then levels off at its carrying capacity, $K_2$. Similar to its effect on the duration of each phase, the initial phage population also determines the maxima attained by the susceptible, infected, and lysed bacterial populations. Since the mutated bacteria are resistant to phage, however, their growth is uninhibited by the phage population. Further, since we let the mutation rate be a constant parameter, $\mu$, mutated populations follow the same sigmoid-curve growth at the exact same time during each experiment, regardless of the phage population. The selective pressure on the susceptible bacteria to mutate might increase as their population declines due to phage, and this is an interesting change to make to our model in the future.

Fig. 4 also describes the phage population in this experiment, where it sharply decreases at the beginning of the experiment when they attach to susceptible and infected bacteria. Then, the phage population steadily increases as virions are produced during lysis of the infected bacteria. It finally stabilizes once all of the susceptible and infected bacteria have died, since phages need to infect those bacteria cells to reproduce and we assume phages cannot "die" during the span of the trial. With the parameters listed in Table 3, the phage population levels off at about 5700 bacteriophage.

The experimental and simulated data reveal, as might be predicted, that increasing the initial number of phage introduced to each microwell plate at the beginning of the experiment makes bacterial populations peak earlier and die off quicker. Toward the latter half of the experiment, however, bacterial populations follow a new S-shaped (sigmoid) growth pattern after being inundated by bacteriophage. The second, somewhat slower growth curve represents resistant (mutant) bacteria which withstand the bacteriophage but exhibit a trade-off between natural growth and phage resistance.

# 5 Discussion

In this work, we developed a system of ordinary differential equations modeling the interaction between bacterial cells and bacteriophages to assess the effect bacterial debris has on optical density readings of bacterial cells in a microwell plate, as well as to determine what assumptions are necessary to accurately represent this interaction. This model captures the different characteristics of susceptible, infected and mutated bacteria. Here, we incorporated a ranked competition model in which susceptible and mutated bacteria are two species competing for resources (nutrients and space in the plate). Due to the cell's loss of fitness associated with bacterial mutations, we assume the susceptible bacteria are the dominant competitors. In addition,

we implemented a density-dependent phage attack rate and accounted for multiple bacteriophages attaching to a single bacterial cell (Han and Smith, 2012; Smith, 2008; Vidurupola, 2018).

Because the $SIP$ subsystem decouples from the $M$ and $L$ equations, it was enough to perform a qualitative analysis of this subsystem to discuss the behavior of the full system. From this analysis, three equilibrium types were obtained. The first is a line of nonisolated bacteria-free equilibra (BFE), in which the bacteriophages completely wipe out the bacterial population. A secondary bifurcation in this line identifies a critical mass of phages ($P = c$) above which a small initial permissive bacterial population will be wiped out. The second is the phage-free equilibrium (PFE). This equilibrium is locally asymptotically stable when the rate at which phages are being produced is less than the rate at which they attach to bacterial cells, allowing the bacterial population to grow to its carrying capacity. Finally, the third equilibrium, and most interesting, the phage-bacterium coexistence equilibrium (COE) occurs when the phage growth rate exceeds the bacterial growth rate, but not by more than than the lysis rate of infected cells (and consequently the rate of production of new phages). This allows the phages to control the bacterial population without an overproduction of phage virions.

Next, we performed a quantitative analysis to determine a set of parameters for our model. Of these parameters, $\epsilon$ represents the contribution of bacterial debris to optical density measurements. We found $\epsilon$ to be 0.43, implying lysed cells contribute 43% as much as live cells. The estimated parameters given in Table 4.1 fit our model to the observed optical density data with a relative error of only 8.5%, versus 11.0% from the best fit without lysed bacteria. Most of this remaining error stems from a slower growth for mutated bacteria at the ends of the trials with fewer initial bacteriophages. Future work should consider what other assumptions could be implemented to capture this phenomenon.

The results of this work confirm that the assumptions made here are important to capture the phage-bacteria dynamics. Some prior mathematical modeling studies introduce a stochastic model, while others implement a system of delay differential equations in order to capture the phage latent period. Though this can produce a more realistic model, it also severely complicates the analysis and computation. Here, we showed that using a deterministic model can produce accurate results while remaining relatively simple to assess. As mentioned above, one limitation of our current model is the inability to accurately capture the slower growth of mutated bacteria near the end of the trials with fewer initial phages. However, since most of the phage-bacteria interaction occurs within the first 5 hours of each experiment (as shown in Fig. 4 and discussed in Section 4.3), we are confident in our parameter estimates. Further, previous studies, such as Cairns *et al.* (2009), also found similar phases of bacterial growth, infection, lysis, and mutation.

Previous studies have found that bacterial debris, particularly from lysed bacteria, can negatively influence a cell's ability to grow within an environment of high nutritional density, despite the opposite effect in an environment with lower nutrition availability (Smakman and Hall, 2022). In future work, our model could be adapted to accurately capture the effect of recently lysed bacteria on bacterial carrying capacity, as the medium used is nutrient-dense. By adding a term for the lysed bacteria

into our carrying capacity, we further reduced the relative error from 8.5% to 5.4% (work not shown), further reinforcing the idea that recent bacterial lysis results in a reduction of carrying capacity for our system. This reduction could be due to clusters of phages or due to the debris itself, possibly causing necrosignaling. Schrag and Mittler (1996), for example, found phage-bacteria coexistence is due to spatial refuges and acquiring phage-resistance, and Simmons *et al.* (2018) found phage motility to be a key factor in determining the survival of bacteriophage in the presence of bacterial biofilms. Additionally, our model could be extended to predict phage efficacy in an *in vivo* setting by incorporating the removal of bacterial cells due to a patient's immune response, as done by Abedon (2008). This extension could lead to important insights in developing treatments to combat infections caused by *P. aeruginosa*. Future work also includes investigating synergistic phage-antibiotic treatments for patients infected by *P. aeruginosa* since phage-resistance may become a major issue similar to antibiotic resistance. Selective pressures placed on *P. aeruginosa* bacteria fighting both bacteriophages and antibiotics could create favorable mutations for defeating *P. aeruginosa* infection (Gurney et al., 2020; Mangalea and Duerkop, 2020; Oechslin et al., 2017).

*Pseudomonas aeruginosa* is a deadly bacterium that is rapidly mutating to become resistant to antibiotic treatments in healthcare settings (Dunham et al., 2010; Sacha et al., 2008; Walsh and Amyes, 2007). Bacteriophages have shown promising signs to be the solution to this problem, but extensive research is needed to implement effective therapies. Mathematical models of the interaction between phages and bacterial cells similar to the one presented in this study are needed to create successful therapies to treat patients afflicted with *Pseudomonas aeruginosa* infections.

# Appendix A Stability Analysis of the Equilibria of $SIP$ Subsystem

In this appendix, we present a detailed existence and stability analysis of the equilibria of Model (3).

## A.1 Fixed Points and Jacobian Matrix

We set $\frac{dS}{dt} = \frac{dI}{dt} = \frac{dP}{dt} = 0$ to determine the fixed points of Model (3) and let $a = \frac{\alpha}{n}, b = \frac{\beta\eta}{\sigma}, c = \frac{\rho}{\alpha}$ to simplify notation. This leads to

$$\{(S^*, I^*, P^*)\} = \Bigg\{(0,0,x), (K_1,0,0),$$
$$\left(K_1\left(\frac{ac-(ab-1)}{a^2bc}\right), K_1\left(\frac{(ac-(ab-1))(ab-1)}{a^2bc}\right), \frac{ab-1}{a}\right)\Bigg\},$$

where $x \geq 0$. We denote the first solution as the bacteria-free equilibria (BFE), the second as the phage-free equilibrium (PFE), and the third as the coexistence equilibrium (COE).

We linearize Model (3) using the Jacobian to evaluate the stability of our fixed points (Strogatz, 2018). To simplify notation, let $h = \frac{\rho}{K_1}$. Then, the Jacobian matrix, where $(S^*, I^*, P^*)$ represents a fixed point, is:

$$\boldsymbol{J}(S^*, I^*, P^*) = \begin{bmatrix} \rho - p(2S^* + I^*) - \alpha P^* & -hS^* & -\alpha S^* \\ \alpha P^* & -\eta & \alpha S^* \\ -\sigma P^* & \beta\eta - \sigma P^* & -\sigma(S^* + I^*) \end{bmatrix}.$$

## A.2 Bacteria-free Equilibria

The bacteria-free equilibria (BFE), $(S^*, I^*, P^*) = (0, 0, x)$ exist in a biologically meaningful sense whenever $x \geq 0$. We examine the nature of the dynamics near this line of equilibria by calculating the eigenvalues of the Jacobian evaluated at each point on the line. This Jacobian matrix becomes:

$$\boldsymbol{J}(0, 0, x) = \begin{bmatrix} \rho - \alpha x & 0 & 0 \\ \alpha x & -\eta & 0 \\ -\sigma x & \eta\beta - \sigma x & 0 \end{bmatrix}.$$

The eigenvalues of this matrix are $\lambda_1 = \rho - \alpha x$, $\lambda_2 = -\eta$, and $\lambda_3 = 0$; this last value reflects the nonisolated nature of the equilibria and makes the Jacobian degenerate (singular). Clearly $\lambda_2 < 0$, but the expression for $\lambda_1$ highlights a special case of the BFE worth noting: $x = \rho/\alpha$, where there is a stability shift in the phage axis. If the number of phages is greater than the ratio of bacterial reproduction rate to the phage interaction rate ($P^* > \rho/\alpha$), then $\lambda_1 < 0$, making the upper portion of the axis a local attractor. However, if the number of phages is less than the ratio of bacterial reproduction rate to the phage interaction rate, then $\lambda_1 > 0$, making the lower portion of the [nonnegative] phage axis act like a saddle point in the $S$ and $I$ dimensions, repelling nearby solutions.

## A.3 Phage-free Equilibrium

The phage-free equilibrium (PFE) occurs when only bacteria are present in the system, and the bacterial population reaches its carrying capacity, $K_1$. We analyze the stability of the system at this point using the eigenvalues of the Jacobian matrix evaluated at the PFE:

$$\boldsymbol{J}(K_1, 0, 0) = \begin{bmatrix} -\rho & -\rho & -\alpha K_1 \\ 0 & -\eta & \alpha K_1 \\ 0 & \eta\beta & -\sigma K_1 \end{bmatrix}.$$

The eigenvalues of this matrix are:

$$\lambda_1 = -\rho,$$

$$\lambda_2 = \frac{1}{2}\left[-(\eta + \sigma K_1) + \sqrt{(\eta + \sigma K_1)^2 + 4\eta K_1(\alpha\beta - \sigma)}\right],$$
$$\lambda_3 = \frac{1}{2}\left[-(\eta + \sigma K_1) - \sqrt{(\eta + \sigma K_1)^2 + 4\eta K_1(\alpha\beta - \sigma)}\right].$$

Since $\lambda_1 < 0$, the PFE is stable if and only if both $\lambda_2 < 0$ and $\lambda_3 < 0$, and, since $\alpha$, $\beta$, $\eta$, $\sigma$, and $K_1$ are positive, this only occurs if $\alpha\beta < \sigma$. Biologically, this means the rate at which new phages are being produced ($\alpha\beta$) must be less than the rate at which phage attach to bacteria ($\sigma$) in the infection process.

## A.4 Coexistence Equilibrium

The coexistence equilibrium (COE) occurs when

$$S = -K_1\frac{(\eta(\alpha\beta - \sigma) - \sigma\rho)}{\alpha\beta\rho} = K_1\left(\frac{ac - (ab-1)}{a^2bc}\right),$$
$$I = -K_1\frac{(\alpha\beta - \sigma)(\eta(\alpha\beta - \sigma) - \sigma\rho)}{\alpha\beta\rho\sigma} = K_1\left(\frac{(ac - (ab-1))(ab-1)}{a^2bc}\right),$$
$$P = \frac{\eta(\alpha\beta - \sigma)}{\alpha\sigma} = \frac{ab-1}{a}.$$

In order for this equilibrium to make sense biologically, each of the values $S, I$, and $P$ must be positive. First, $P > 0$ implies $\alpha\beta - \sigma > 0$. Then, from $S > 0$ and $I > 0$, we have $\sigma\rho > \eta(\alpha\beta - \sigma) > 0$. For this equilibrium to exist meaningfully, the following compound inequality must be satisfied: $0 < \eta(\alpha\beta - \sigma) < \sigma\rho$. Biologically, this means that in order for the population of phage to survive, they need to be produced at a faster rate than they attach to susceptible or infected bacteria. For the bacterial populations to survive, the rates of the net bacterial population growth must be higher than the net growth of the phage population.

The Jacobian evaluated at this point simplifies to

$$\boldsymbol{J}(COE) = \begin{bmatrix} -\frac{\alpha cd}{ab} & -\frac{\alpha cd}{ab} & -\alpha K_1\frac{d}{ab} \\ \eta(ab-1) & -\eta & \eta a K_1\frac{d}{ab} \\ -\sigma\left(\frac{ab-1}{a}\right) & \frac{\sigma}{a} & -\sigma K_1 d \end{bmatrix},$$

where $d = \frac{ac-(ab-1)}{ac}$. Note that $d > 0$ if, and only if, $\sigma\rho > \eta(\alpha\beta - \sigma)$, which is an existence condition. Because the eigenvalues of this matrix are difficult to compute and interpret, to analyze stability at this point we use the 3D Routh-Hurwitz criterion, which states that this equilibrium is LAS iff the coefficients of the characteristic polynomial of the Jacobian evaluated at this point, $p_J(\lambda) = \lambda^3 + a_2\lambda^2 + a_1\lambda + a_0$, satisfy the following conditions: $a_0 > 0, a_2 > 0$ and $a_1a_2 - a_0 > 0$.

With some algebra, we find that $a_2 = \frac{\alpha cd}{ab} + \eta + dK_1\sigma$. Notice that each parameter in this equation is positive, meaning $a_2 > 0$. Next, we examine the coefficient $a_0 = \alpha cd^2\eta K\sigma\left(\frac{ab-1}{ab}\right)$, which is positive if $ab > 1$. This is equivalent to $\alpha\beta > \sigma$, which is

part of the existence criterion of this fixed point. Therefore, $a_0 > 0$. Lastly, we look into

$$a_1a_2 - a_0 = -\frac{(ab-1)\alpha cd^2\eta K_1\sigma}{ab} + \left(\frac{\alpha cd}{ab} + \eta + dK_1\sigma\right)\left(\alpha cd\eta + \frac{\alpha cd^2K_1\sigma}{ab} + [(ab-1)dK_1\sigma]\left(\frac{\eta}{ab} - \frac{\alpha}{a^2b}\right)\right).$$

With some algebra, this reduces to

$$a_1a_2 - a_0 = \frac{1}{(ab)^2}acd\eta\left[(ab-1)(ab+acd)\eta^2 + acd\eta(\eta + dK_1\sigma) + ab(\eta + dK_1\sigma)^2\right],$$

which is always positive since $d > 0$ and $ab - 1 > 0$ by the above discussion. Thus, by the Routh-Hurwitz criteria, the coexistence equilibrium is stable whenever it exists. Note, a transcritical bifurcation must therefore occur at $\alpha\beta = \sigma$, since the coexistence equilibrium is stable for $\alpha\beta > \sigma$ and unstable otherwise, while the phage-free equilibrium is stable for $\alpha\beta < \sigma$ and unstable otherwise.

### A.5 Bifurcation Analysis

As noted, the coexistence equilibrium only occurs when the compound inequality $0 < \eta(\alpha\beta - \sigma) < \sigma\rho$ is satisfied. If the left inequality is not satisfied, i.e., $\alpha\beta < \sigma$, then the stability passes from the coexistence equilibrium to the phage-free equilibrium (indeed, at the transcritical bifurcation $\alpha\beta = \sigma$ the COE passes outside the nonnegative state space through the PFE). If the right inequality is not satisfied, i.e., $\eta(\alpha\beta - \sigma) > \sigma\rho$, then the COE has instead passed outside the state space through the "threshold" BFE $(0, 0, \rho/\alpha)$; since the PFE is unstable, solutions should approach the upper portion $(P > \rho/\alpha)$ of the BFE line. The bifurcation delimiting this mode is also transcritical in nature, although the threshold BFE involved is never properly asymptotically stable.

In summary, the two bifurcations divide parameter space into three modes of operation: For $0 < ab < 1$, phages do a poor job of replicating while bacteria are typically able to persist; the PFE is LAS, but the upper portion of the BFE line is also locally attracting. For $1 < ab < 1 + ac$, both bacteria and phages are typically able to persist; the COE is LAS, but the upper portion of the BFE line remains locally attracting. Finally, for $ab > 1 + ac$, the bacteria are slowly wiped out by the phages, and the only attractor is the upper BFE line.

## Declarations

**Funding.** This work was supported by the US National Science Foundation under Grant No. DMS-2230790. Initial data generation was supported in part by a grant from the Department of Defense to MSA (eBRAP #21000310).

**Competing Interests.** The authors declare that they have no known competing financial interests or personal relationships that could have appeared to influence the work reported in this paper.

**Ethics approval and consent to participate.** Not applicable.

**Consent for publication.** Not applicable.

**Data and Code availability.** Data sets generated for this study and a code to replicate the analysis supporting the findings of this manuscript are available on the Harvard Dataverse at https://doi.org/10.7910/DVN/9IRTRK.

**Materials availability.** Not applicable.

**Author Contributions.** Conceptualization, H.V.K. and C.K.; methodology, S.R., A.C., D.G., C.P., A.L., E.R., C.K., and H.V.K.; software, S.R., A.C., D.G., C.P., and A.L.; formal analysis, A.C., D.G., C.P., A.L., E.R., and C.K.; investigation, M.A., J.S.; writing—original draft preparation, S.R., A.C., D.G., C.P., A,L., and C.K.; writing—review and editing, H.V.K., C.K., S.R., A.C., D.G., C.P., M.A., and J.S.; visualization, A.C., D.G., and C.P.; supervision, H.V.K. and C.K.; funding acquisition, H.V.K., C.K., S.R., and M.A.

# References


Abedon, S.T. (ed.): Bacteriophage Ecology: Population Growth, Evolution, and Impact of Bacterial Viruses vol. 15, pp. 31–47. Cambridge University Press, London, UK (2008)

Alharbi, M.H., Kribs, C.M.: A mathematical modeling study: Assessing impact of mismatch between influenza vaccine strains and circulating strains in Hajj. Bull Math Biol **84**(8) (2022)

Aksyuk, A.A., Leiman, P.G., Kurochkina, L.P., Shneider, M.M., Kostyuchenko, V.A., Mesyanzhinov, V.V., Rossmann, M.G.: The tail sheath structure of bacteriophage T4: a molecular machine for infecting bacteria. EMBO J **28**(7), 821–829 (2009)

Bayer, M.: Adsorption of bacteriophages to adhesions between wall and membrane of Escherichia coli. J Virol **2**(4), 346–356 (1968)

Barrangou, R., Fremaux, C., Deveau, H., Richards, M., Boyaval, P., Moineau, S., Romero, D.A., Horvath, P.: CRISPR provides acquired resistance against viruses in prokaryotes. Science **315**(5819), 1709–1712 (2007)

Beal, J., Farny, N.G., Haddock-Angelli, T., Selvarajah, V., Baldwin, G.S., Buckley-Taylor, R., Gershater, M., Kiga, D., Marken, J., Sanchania, V., Sison, A., Workman, C.T., Interlab Study Contributors: Robust estimation of bacterial cell count from optical density. Commun Biol **3**(1), 512 (2020)

Betts, A., Kaltz, O., Hochberg, M.E.: Contrasted coevolutionary dynamics between a bacterial pathogen and its bacteriophages. Proc Natl Acad Sci USA **111**(30), 11109–11114 (2014)

Bédard, E., Prévost, M., Déziel, E.: *Pseudomonas aeruginosa* in premise plumbing of large buildings. Microbiologyopen **5**(6), 937–956 (2016) https://doi.org/10.1002/mbo3.391

Burgener, E.B., Sweere, J.M., Bach, M.S., Secor, P.R., Haddock, N., Jennings, L.K., Marvig, R.L., Johansen, H.K., Rossi, E., Cao, X., *et al.*: Filamentous bacteriophages are associated with chronic Pseudomonas lung infections and antibiotic resistance in cystic fibrosis. Sci Transl Med **11**(488), 9748 (2019)

Booth, S., Van Tassell, R., Johnson, J., Wilkins, T.: Bacteriophages of bacteroides. Rev Infect Dis **1**(2), 325–336 (1979)

Blanchard, A.C., Waters, V.J.: Microbiology of cystic fibrosis airway disease. In: Seminars in Respiratory and Critical Care Medicine, vol. 40, pp. 727–736 (2019). Thieme Medical Publishers

Chegini, Z., Khoshbayan, A., Taati Moghadam, M., Farahani, I., Jazireian, P., Shariati, A.: Bacteriophage therapy against Pseudomonas aeruginosa biofilms: a review. Ann Clin Microbiol Antimicrob **19**, 1–17 (2020)

Clokie, M.R., Millard, A.D., Letarov, A.V., Heaphy, S.: Phages in nature. Bacteriophage **1**(1), 31–45 (2011)

Cairns, B.J., Timms, A.R., Jansen, V.A., Connerton, I.F., Payne, R.J.: Quantitative models of in vitro bacteriophage–host dynamics and their application to phage therapy. PLoS Pathog **5**(1), 1000253 (2009)

Crone, S., Vives, M., Kvich, L., Saunders, A., Malone, M., Nicolaisen, M., Martínez-García, E., Rojas-Acosta, C., Gomez-Puerto, M.C., Calum, H., Whiteley, M., Kolter, R., Bjarnsholt, T.: The environmental occurrence of Pseudomonas aeruginosa. APMIS **128** (2019) https://doi.org/10.1111/apm.13010

Dunham, S., McPherson, C., Miller, A.: The relative contribution of efflux and target gene mutations to fluoroquinolone resistance in recent clinical isolates of Pseudomonas aeruginosa. Eur J Clin Microbiol Infect Dis **29**, 279–288 (2010)

Emmanouilidou-Arseni, A., Koumentakou, I.: Viability of Pseudomonas aeruginosa. J Bacteriol **87**(5), 1253 (1964)

Egido, J.E., Toner-Bartelds, C., Costa, A.R., Brouns, S.J.J., Rooijakkers, S.H.M., Bardoel, B.W., Haas, P.-J.: Monitoring phage-induced lysis of gram-negatives in real time using a fluorescent DNA dye. Sci Rep **13**(856) (2023)

Fink, J.W., Held, N.A., Manhart, M.: Microbial population dynamics decouple growth response from environmental nutrient concentration. Proc Natl Acad Sci USA **120**(2), 2207295120 (2023)

Gurney, J., Brown, S.P., Kaltz, O., Hochberg, M.E.: Steering phages to combat bacterial pathogens. Trends Microbiol **28**(2), 85–94 (2020)

Han, Z., Smith, H.L.: Bacteriophage-resistant and bacteriophage-sensitive bacteria in a chemostat. Math Biosci Eng **9**(4), 737–765 (2012)

Hynes, A.P., Villion, M., Moineau, S.: Adaptation in bacterial CRISPR-Cas immunity can be driven by defective phages. Nat Commun **5**(1), 4399 (2014)

Kadurugamuwa, J.L., Beveridge, T.J.: Bacteriolytic effect of membrane vesicles from Pseudomonas aeruginosa on other bacteria including pathogens: conceptually new antibiotics. J Bacteriol **178**(10), 2767–2774 (1996)

Kim, D.-j., Chung, S.-g., Lee, S.-h., Choi, J.-w.: Relation of microbial biomass to counting units for Pseudomonas aeruginosa. Afr J Microbiol Res **6**(21), 4620–4622 (2012)

Kwiatek, M., Parasion, S., Rutyna, P., Mizak, L., Gryko, R., Niemcewicz, M., Olender, A., Łobocka, M.: Isolation of bacteriophages and their application to control Pseudomonas aeruginosa in planktonic and biofilm models. Res Microbiol **168**(3), 194–207 (2017)

Kokjohn, T.A., Sayler, G.S.: Attachment and replication of Pseudomonas aeruginosa bacteriophages under conditions simulating aquatic environments. Microbiology **137**(3), 661–666 (1991)

Kauppinen, A., Siponen, S., Pitkänen, T., Holmfeldt, K., Pursiainen, A., Torvinen, E., Miettinen, I.: Phage biocontrol of Pseudomonas aeruginosa in water. Viruses **13** (2021)

Lewenza, S., Abboud, J., Poon, K., Kobryn, M., Humplik, I., Bell, J.R., Mardan, L., Reckseidler-Zenteno, S.: Pseudomonas aeruginosa displays a dormancy phenotype during long-term survival in water. PloS One **13**(9), 0198384 (2018)

LiPuma, J.J.: The changing microbial epidemiology in cystic fibrosis. Clin Microbiol Rev **23**(2), 299–323 (2010)

Łusiak-Szelachowska, M., Weber-Dąbrowska, B., Żaczek, M., Borysowski, J., Górski, A.: The presence of bacteriophages in the human body: good, bad or neutral? Microorganisms **8**(12), 2012 (2020)

Matlock, B.C.: Differences in bacterial optical density measurements between uv-visible spectrophotomers. Therm Sci **52236** (2017)

MathWorks: MATLAB Version: 24.1.0 (R2024a). Natick, Massachusetts, United States (2024). https://www.mathworks.com

Mangalea, M.R., Duerkop, B.A.: Fitness trade-offs resulting from bacteriophage resistance potentiate synergistic antibacterial strategies. Infect Immun **88**(7), 10–1128 (2020)

Malhotra, S., Hayes Jr, D., Wozniak, D.J.: Cystic fibrosis and Pseudomonas aeruginosa: the host-microbe interface. Clin Microbiol Rev **32**(3), 10–1128 (2019)

Ndongmo Teytsa, H., Tsanou, B., Bowong, S., Lubuma, J.M.: Bifurcation analysis of a phage-bacteria interaction model with prophage induction. Math Med Biol **38**(1), 28–58 (2021)

Oechslin, F., Piccardi, P., Mancini, S., Gabard, J., Moreillon, P., Entenza, J.M., Resch, G., Que, Y.-A.: Synergistic interaction between phage therapy and antibiotics clears Pseudomonas aeruginosa infection in endocarditis and reduces virulence. J Infect Dis **215**(5), 703–712 (2017)

Orlova, E.V.: How viruses infect bacteria? EMBO J **28**(7), 797–798 (2009)

Pachori, P., Gothalwal, R., Gandhi, P.: Emergence of antibiotic resistance Pseudomonas aeruginosa in intensive care unit; a critical review. Genes Dis **6**(2), 109–119 (2019)

Schroth, M., Cho, J., Green, S., Kominos, S.: Epidemiology of Pseudomonas aeruginosa in agricultural areas*. J Med Microbiol **67**, 1191–1201 (2018) https://doi.org/10.1099/jmm.0.000758

Schmidt, M.: An interior-point method for nonlinear optimization problems with locatable and separable nonsmoothness. EURO Journal on Computational Optimization **3**, 309–348 (2015)

Simmons, E.L., Drescher, K., Nadell, C.D., Bucci, V.: Phage mobility is a core determinant of phage–bacteria coexistence in biofilms. ISME J **12**(2), 532–543 (2018)

Serralta, J.: Isolation and characterization of a novel bacteriophage for Pseudomonas aeruginosa. Master of Science thesis, University of North Texas Health Science Center at Fort Worth (2023). 61 pages

Sinha, S., Grewal, R.K., Roy, S.: Modeling phage–bacteria dynamics. Immunoinformatics (Amst), 309–327 (2020)

Smakman, F., Hall, A.R.: Exposure to lysed bacteria can promote or inhibit growth of neighboring live bacteria depending on local abiotic conditions. FEMS Microbiol Ecol **98**(2), 011 (2022)

Schrag, S., Mittler, J.: Host-parasite coexistence: the role of spatial refuges in stabilizing bacteria-phage interactions. Am Nat **148**(2), 348–377 (1996)

Smith, H.L.: Models of virulent phage growth with application to phage therapy. SIAM J Appl Math **68**(6), 1717–1737 (2008)

Solomon, S.L., Oliver, K.B.: Antibiotic resistance threats in the United States: stepping back from the brink. Am Fam Physician **89**(12), 938–941 (2014)

Smith, H.L., Trevino, R.: Bacteriophage infection dynamics: multiple host binding sites. Math Model Nat Phenom **4**(6), 109–134 (2009)

Strogatz, S.H.: Nonlinear Dynamics and Chaos: with Applications to Physics, Biology, Chemistry, and Engineering. CRC press, Boca Raton, USA (2018)

Sacha, P., Wieczorek, P., Hauschild, T., Zórawski, M., Olszańska, D., Tryniszewska, E.: Metallo-beta-lactamases of Pseudomonas aeruginosa–a novel mechanism resistance to beta-lactam antibiotics. Folia Histochem Cytobiol **46**(2), 137–142 (2008)

Tacconelli, E., Carrara, E., Savoldi, A., Harbarth, S., Mendelson, M., Monnet, D.L., Pulcini, C., Kahlmeter, G., Kluytmans, J., Carmeli, Y., *et al.*: Discovery, research, and development of new antibiotics: the WHO priority list of antibiotic-resistant bacteria and tuberculosis. Lancet Infect Dis **18**(3), 318–327 (2018)

Thieme, H.R.: Convergence results and a Poincaré-Bendixson trichotomy for asymptotically autonomous differential equations. J Math Biol **30**(7), 755–763 (1992)

Vidurupola, S.W.: Analysis of deterministic and stochastic mathematical models with resistant bacteria and bacteria debris for bacteriophage dynamics. Appl Math Comput **316**, 215–228 (2018)

Vincent, J.-L., Rello, J., Marshall, J., Silva, E., Anzueto, A., Martin, C.D., Moreno, R., Lipman, J., Gomersall, C., Sakr, Y., *et al.*: International study of the prevalence and outcomes of infection in intensive care units. JAMA **302**(21), 2323–2329 (2009)

Walsh, F., Amyes, S.: Carbapenem resistance in clinical isolates of Pseudomonas aeruginosa. J Chemother **19**(4), 376–381 (2007)

Wright, R.C., Friman, V.-P., Smith, M.C., Brockhurst, M.A.: Cross-resistance is modular in bacteria–phage interactions. PLoS Biol **16**(10), 2006057 (2018)

Weitz, J.S., Hartman, H., Levin, S.A.: Coevolutionary arms races between bacteria and bacteriophage. Proc Natl Acad Sci USA **102**(27), 9535–9540 (2005)

Webb, J.S., Thompson, L.S., James, S., Charlton, T., Tolker-Nielsen, T., Koch, B., Givskov, M., Kjelleberg, S.: Cell death in Pseudomonas aeruginosa biofilm development. J Bacteriol **185**(15), 4585–4592 (2003)

Yang, L., Haagensen, J.A., Jelsbak, L., Johansen, H.K., Sternberg, C., Høiby, N., Molin, S.: In situ growth rates and biofilm development of Pseudomonas aeruginosa populations in chronic lung infections. J Bacteriol (2008)

Zhang, X., Wang, Y., Guo, J., Yu, Y., Li, J., Guo, Y., Liu, C.: Comparing two functions for optical density and cell numbers in bacterial exponential growth phase. J Pure Appl Microbiol **9**(1), 299–305 (2015)